Coupling and Damping Effects on the Dynamics of Submerged Expanded Tubes in Borehole Wells

A Karrech[*a] and AC Seibi[b]

[a]*School of Civil and Resources Engineering, The University of Western Australia, Crawley, Western Australia, Australia*
[b]*Mechanical Engineering Department, Petroleum Institute, Abu Dhabi, United Arab Emirates*

Abstract: Hydraulic expansion of submerged tubes is accomplished by propelling a mandrel through it using differential pressure. This process deforms the tube beyond its elastic limit. Toward the end of the expansion process, the mandrel pops out of the tube resulting in displacement, stress, and pressure waves propagating through the system. A mathematical model has been developed to describe the dynamics of the tube-fluid system due to the pop-out phenomenon. The model takes into consideration the coupling effect between fluids and the structure, as well as the inherent system damping of its response. An analytical solution describing the wave propagation in the tube-fluid system was obtained. The model identified the potential failure locations and showed that the inherent system damping reduced the chances of failure but could not eliminate it completely. In addition, it showed that the coupling effect was more prominent in the tube as compared to the outer and inner fluids. Furthermore, a sensitivity analysis was conducted in order to investigate the effect of the geometrical and material properties on the response. The sensitivity analysis showed that the coupling effect vanished with the increase in tube stiffness and reached an asymptotic value with an increase in formation stiffness.

Keywords: Pop-out, Expansion, Stress/pressure waves, Coupling, Damping

آثار الاقتران و التخميد على ديناميكيات الأنابيب الممددة الغائصة في الآبار

علي كرش أ* و عبدالنور س سيبي ب

الملخص: يتم إنجاز عملية التمديد الهيدروليكي للأنابيب المغمورة عن طريق دفع جسم مغزلي الشكل من خلال تلك الأنابيب، وذلك باستخدام الفرق في الضغط. حيث يعمل الجسم المغزلي من خلال حركته داخل الأنبوب الى إحداث تشوهات تفوق الحد الأقصى لمرونة مادة الأنبوب مما يكسبه حجما جديدا. ولكن في نهاية عملية التمديد تحدث عملية اندفاع للجسم المغزلي أثناء خروجه من الأنبوب مما يسبب إحداث موجات نزوح وتوتر وضغط تنتشر في النظام. ومن أجل دراسة هذه الظاهرة فقد تم تطوير نموذج رياضي لوصف ديناميكيات النظام المكون من الأنبوب والسوائل المحيطة به، ويأخذ هذا النموذج بعين الاعتبار تأثيرالاقتران بين السوائل وبنية الأنبوب فضلا عن تأثير عامل التخميد للنظام على تأثير هذه العوامل. وباستخدام هذا النموذج تم الحصول على نتائج تحليلية تصف الموجات المنتشرة في النظام والتي بدورها ساهمت في تحديد مواقع الفشل المحتملة، كما تبين من خلال هذه النتائج بأن عامل التخميد التابع للنظام يقلل من فرص الفشل، ولكنه غير قادر على القضاء عليها تماما. كما تبين أيضا بأن تأثير الاقتران كان أكثر بروزا على الأنبوب نفسه بالمقارنة مع السوائل الخارجية والداخلية المحيطة به. وإضافة على ذلك، فقد تم إجراء تحليل الحساسية من أجل دراسة تأثير الخصائص الهندسية وكذلك مواد الأنبوب على الاستجابة حيث تبين بأن تأثير الاقتران يختفي مع الزيادة في صلابة الأنبوب ويصل إلى قيمة مقاربة مع الزيادة في صلابة البنية المحيطة.

المفردات المفتاحية: الاندفاع المفاجىء، التمدد، موجات الإجهاد/الضغط، الاقتران، التخميد

---

*Corresponding author's e-mail: ali.karrech@uwa.edu.au

1. Introduction

Solid expandable tubular (SET) technology is a down-hole process consisting of expanding the diameter of a tube by pushing or pulling a mandrel through it. Recent interest and further research in SET will be able to provide solutions for many unsolvable problems having to do with well drilling and completion, such as extended reach applications, mono-diameter wells, cost- effective repair of damaged zones and the conservation of hole-sizes.

The principle behind SET is simple. A mechanical expansion device, known as a mandrel, is pushed through the tube hydraulically by back pressure across the mandrel. The forward movement of the mandrel expands the tube to the required diameter.

The first SET test was performed at Royal Dutch Shell in The Hague (Fillipov *et al*. 1999). The test results were encouraging and paved the way for significant research work in this field. Recently, there has been an increase in applications in well engineering due to their many successes in deep water applications as well as its cost effectiveness in solving many long standing problems faced during the construction and operation of wells (Owoeye *et al*. 2000). Most of the researchers have focused their efforts on determining the power required for down-hole tube expansion and its effect on mechanical properties including burst and collapse strengths (Fillipov *et al*. 1999; Mark *et al*. 2000). Ruggier *et al*. (2001) attributed the decrease in collapse pressure to the length and thickness variation, the Bauschinger effect, and residual stresses. Stewart *et al*. (1999) conducted a laboratory test on a 3.5-inch outer diameter tube and showed that the elongation at fracture and uniform strain decreased, while the yield and ultimate tensile strength increased. Limited successful applications of SET in well construction and remediation were reported by Daigle *et al*. (2000). Due to the complexity of the process, the researchers have focused their effort only on determining the power required for down-hole and simulated expansion, and post-expansion behavior using the finite element method. Pervez *et al*. (2005) used a non-linear explicit finite element analysis to study the effects of expansion ratio, friction coefficient, and mandrel angle on tube expansion. It was found that for small conical angles in mandrels and in large expansion ratios, the failure could not be avoided even at low values of friction coefficient. In a subsequent study, Pervez *et al*. (2005) concluded that the tube wall thickness decreased with an increase in mandrel angle, expansion ratio, and friction coefficient. The tube length often shortened for expansion under tension for most of the loading mechanisms, but it elongated at high drawing force.

During the hydraulic expansion process, elastic energy is stored in the tube, and in inner and outer fluids. When the mandrel pops out of the tube, the stored energy is suddenly released resulting in an excitation of the whole assembly. This dynamic condition is called the pop-out phenomenon. Nothing has been found in the literature that specifically addresses the pop-out phenomenon. The authors have developed a mathematical model without damping effects to predict the system response as well as the propagation of displacement, pressure, and stress waves in the tube, and in the inner and outer fluids (Karrech *et al*. 2004; Pervez *et al*. 2006). It was found that the three mediums interact with each other immediately after the pop-out phenomenon takes place, where a small disturbance in one medium influences the others. When the tube is purely elastic, the effect of the outer fluid on the inner fluid is substantially higher (Seibi *et al*. 2004). This reduces significantly if the tube material is elastic perfectly plastic. Aarrestad *et al*. (1986) studied a similar problem regarding the dynamics of submerged drill strings. In this study, the damping effects were included but the coupling between the drill string and the fluid were ignored. It was found that frequency-dependent damping more accurately responded than constant damping when compared with experimental results. For the same problem, Lea (1996) carried out a modal analysis including the coupling effect between the drill string and fluid. This work neglected damping effects. Wang and Bloom (1999) investigated the effect of geometry on the natural frequencies and damping ratios of an inclined submerged tube.

In general, an oscillating system dissipates energy while vibrating. Therefore, damping is considered one of the most important characteristics of the system unless it is not desirable by design. It is certainly useful in SET, where it may limit the resonant amplitudes of the structures and drive system, stabilize instruments and sub-systems, or reduce the danger of tube failure. Virtually all phases of the response of tube-fluid system are affected by the damping, yet no efforts have been made for their proper characterization.

The primary goal of this work was to predict the system response and determine the coupling effects between the propagating waves in the tube and its inner and outer fluids while considering the inherent damping present in the system. Due to the difficulties in mathematically representing a real damping mechanism, a proportional damping approximation has been employed here. The influence of formation stiffness, tube material properties, and fluid characteristics on coupling effects is also investigated here.

(a) Expansion Process

(b) Pop Out Phenomenon
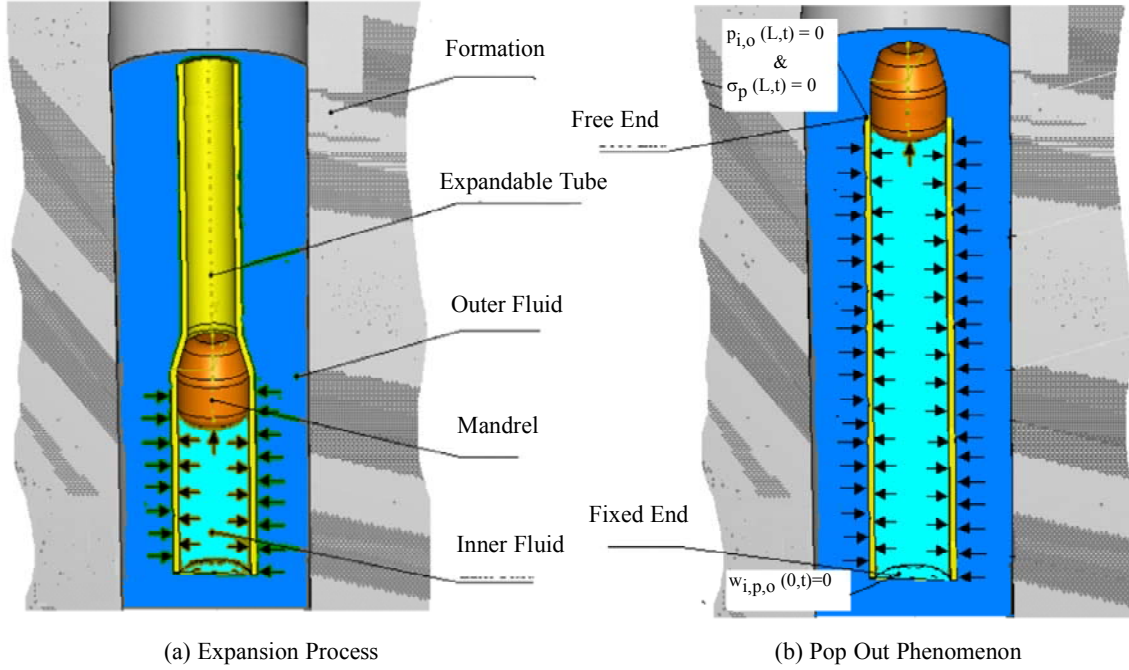
Figure 1. Schematic diagram of tube expansion and boundary conditions

2. Problem Formulation

The tube-fluid system to be studied consists of a down-hole expanded tube, a mandrel pumped through it, and fluids from inside and outside as shown in Fig. 1. It is assumed that

* the tube, and inner and outer fluid layers are uniform and homogeneous;
* the formation is impermeable;
* the steady state fluid velocity is low compared to the axial wave propagation speed;
* all waves are monochromatic and wavelengths are long as compared to the borehole diameter, and
* the tube material is elastic perfectly plastic as the tube is already plastically deformed due to the expansion process.

During the expansion process, the tube, with inner and outer post-expansion radii of r_i and r_o, respectively, is subjected to an inner pressure, p_i and an outer pressure, p_o. When the mandrel leaves the tube, the inner pressure and the axial stress in the tube suddenly drop to zero. During the expansion process, elastic energy is being stored in the fluid and the tube depending on its dimensions and mechanical properties.

2.1 Coupled Equations of Motion

Using the above-mentioned assumptions, the continuity of the mass and momentum of the fluids as well as the equations of motion for the tube-fluid system, the wave equations associated with the inner fluid, elastic perfectly plastic tube, and the outer fluid, respectively, can be expressed as

$$\frac{B_i}{\rho_i}\frac{\partial^2 w_i}{\partial z^2} = \left(1+\frac{(4\nu^2+2\nu-1)B_i}{E}\right)\frac{\partial^2 w_i}{\partial t^2} + \\ 2\nu\frac{\rho_p}{\rho_i}\frac{B_i}{E}\frac{\partial^2 w_p}{\partial t^2} - 4\nu^2\frac{B_i}{E}\frac{\rho_o}{\rho_i}\frac{\partial^2 w_o}{\partial t^2} \quad (1)$$

$$\frac{E}{\rho_p}\frac{\partial^2 w_p}{\partial z^2} = \frac{\partial^2 w_p}{\partial t^t} - \frac{2\nu\rho_o}{\rho_p}\frac{\partial^2 w_o}{\partial t^2} \quad (2)$$

$$\frac{B_o}{\rho_o}\frac{\partial^2 w_o}{\partial z^2} = \frac{2r_o^2\nu}{(r_o^2-r_b^2)}\frac{B_o}{E}\frac{\rho_p}{\rho_o}\frac{\partial^2 w_p}{\partial t^2} + \\ \left(1+\frac{B_o}{G}\frac{r_b^2}{(r_b^2-r_o^2)}+\frac{B_o}{E}\frac{2(1-\nu)r_o^2}{(r_b^2-r_o^2)}\right)\frac{\partial^2 w_o}{\partial t^2} \quad (3)$$

The derivation of these governing differential equations is shown in the Appendix. The coupling effect is mainly dependent on the cross sectional dynamic change and the material properties such as densities, fluid's bulk modulus, the formation shear modulus, and the tube's elastic constants. The above-mentioned equations of motion can be written in a matrix form where the off-diagonal terms describe the coupled behavior of wave propagation in the three mediums.

$$\mathbf{A}\frac{\partial^2}{\partial t^2}\begin{Bmatrix} w_i \\ w_p \\ w_o \end{Bmatrix} - \frac{E}{\rho_p}\mathbf{I}\frac{\partial^2}{\partial z^2}\begin{Bmatrix} w_i \\ w_p \\ w_o \end{Bmatrix} = \begin{Bmatrix} 0 \\ 0 \\ 0 \end{Bmatrix} \qquad (4)$$

where $\mathbf{w} = \{w_i \; w_p \; w_o\}^T$ represents the displacement vector in the three mediums. $\mathbf{A}$ is the matrix of known coefficients and $\mathbf{I}$ is the 3 x 3 identity matrix. Using the transformation $\mathbf{\Psi} = \mathbf{w}e^{-i(\varpi t + KZ)}$, Eqn. 4 can be expressed as a linearized eigenvalue problem as follows:

$$\mathbf{A}\frac{\partial^2}{\partial t^2}\begin{Bmatrix} \psi_i \\ \psi_p \\ \psi_o \end{Bmatrix} + \mathbf{B}\begin{Bmatrix} \psi_i \\ \psi_p \\ \psi_o \end{Bmatrix} = \mathbf{0} \qquad (5)$$

where the matrix $\mathbf{B}$ is defined as $\mathbf{B} = \kappa^2 \rho_p^{-1} E\mathbf{I}$ and $\mathbf{\Psi} = \{\psi_i \; \psi_p \; \psi_o\}^T$ is the vector of the generalized axial displacements. The solution of Eqn. 5 gives three eigenvalues, λ_n, corresponding to three wave propagation modes. Each eigenvalue defines a wave-number κ_n as

$$\kappa_n = \sqrt{\frac{\varpi_n^2 \rho_p \lambda_n}{E}} = \frac{\varpi_n}{s_n} \qquad n = i, p, o \qquad (6)$$

where the subscripts 'i', 'p' and 'o' refer to the inner fluid, the tube, and the outer fluid, respectively. The terms ϖ_n and S_n denote the angular frequencies and wave propagation speeds for the tube, and the inner and outer fluids.

2.2 Damping Approximation

The damping effects have been neglected while deriving the equation of motion (Eqn. 4) and the eigenvalue problem (Eqn. 5) of the tube-fluid system. Although neglecting damping simplifies the derivation, it jeopardizes complete understanding of the dynamics of the system. In order to obtain relevant results, damping must be taken into consideration in determining the system response in terms of displacement, pressure, and stress waves through the three mediums. In general, the damping force in a dynamic equilibrium equation is proportional to velocity. Hence, augmenting Eqn. 5 with a damping force term gives

$$\mathbf{A}\frac{\partial^2}{\partial t^2}\begin{Bmatrix} \psi_i \\ \psi_p \\ \psi_o \end{Bmatrix} + \mathbf{D}\frac{\partial}{\partial t}\begin{Bmatrix} \psi_i \\ \psi_p \\ \psi_o \end{Bmatrix} + \mathbf{B}\begin{Bmatrix} \psi_i \\ \psi_p \\ \psi_o \end{Bmatrix} = \mathbf{0} \qquad (7)$$

Where $\mathbf{D}$ represents the damping matrix. The ways in which the tube-fluid system may be damped are diverse and can incorporate many different kinds of mechanisms. For instance, the tube vibration can be damped due to the viscous effects of the surrounding fluids. In addition, the visco-elastic effect of the solid mediums further enhances damping. According to Apostal *et al.* (1990), the damping matrix of a submerged drill-string in a borehole contains terms based on the effect of proportional, structural, and viscous damping. The effect of Rayleigh or proportional damping on the bottom-hole assembly (BHA) vibrational response is described by $\mathbf{D}_r = \alpha_o \mathbf{A} + \alpha_1 \mathbf{B}$, where α_o and α_1 are proportionality coefficients. The structural damping, which is assumed to be proportional to the displacement but in phase with the velocity of a harmonically oscillating BHA, is decomposed into two separate terms: $\mathbf{D}_s = \alpha_2 \mathbf{B} + \alpha_3 \mathbf{B}_c$. The first term characterizes the behavior of the BHA alone while the second term represents the possible contact between the structure and the borehole, and $\mathbf{B}_c$ is the equivalent contact (or formation) stiffness matrix. Also, the viscous damping describes the energy dissipation by laminar fluid friction. Aarrestad *et al.* (1986) showed that the fluid viscous damping was negligible as compared to the breathing effects (*ie.* the effect of the propagating waves on the environment due to the radial contraction of the tube); hence, it can be ignored in the present system. In addition, the tube did not come in direct contact with the formation, as the structure did not experience bending due to pop-out. Therefore, the damping of the system under consideration can be described by a damping matrix, which is proportional to the equivalent mass and stiffness matrices:

$$\mathbf{D} = \alpha_o \mathbf{A} + \alpha_1 \mathbf{B} \qquad (8)$$

The constants α_o and α_1 satisfy the relation

$$\xi = \frac{a_0}{2\varpi} + \frac{a_1\varpi}{2} \qquad (9)$$

where ξ is the damping ratio and ϖ is the natural frequency of the system.

Using Eqn. 9 for the first two modes of vibration gives

$$\xi_1 = \frac{a_0}{2\omega_1} + \frac{a_1\omega_1}{2} \quad \xi_2 = \frac{a_0}{2\omega_2} + \frac{a_1\omega_2}{2} \qquad (10)$$

The dynamic response is essentially governed by the lower modes. Therefore, in the above equation, the constants α_o and α_1 can be determined once the frequencies of the first two modes and their corresponding damping ratios are known. However, the values that bracket the likely range of frequencies of interest can also be used for certain applications.

Fossen and Johansen (2002) performed an experiment on a similar submerged cylinder in a frame to determine the natural frequencies and damping ratios. The tests for different fluids were carried out at Institutt for Teknisk Kybernetikk at Norges Teknisk-Naturvitenskapelige Universitet (NTNU). These tests experimentally determined the damping ratios used in Eqn. 10 along with the first two fundamental frequencies of the system to calculate unknown constants α_o and α_1.

3. Solution of Governing Equations

The orthogonality properties of the undamped mode shapes are used to decouple the equations of motion (Eqn. 7). Using the transformation $\boldsymbol{\psi} = \boldsymbol{\Phi}_\mathbf{y}$, Eqn. 7 reduces to

$$\boldsymbol{\Phi}^\mathbf{T}\mathbf{A}\boldsymbol{\Phi}\ddot{\mathbf{y}} + \boldsymbol{\Phi}^\mathbf{T}\mathbf{D}\boldsymbol{\Phi}\dot{\mathbf{y}} + \boldsymbol{\Phi}^\mathbf{T}\mathbf{B}\boldsymbol{\Phi}\,\mathbf{y} = \mathbf{0} \qquad (11)$$

where $\boldsymbol{\Phi}$ is the modal matrix consisting of independent mode shapes of the associated undamped system. Use of the orthogonality condition reduces the coefficients in the above equation to

$$\phi_n^T \mathbf{A} \phi_n = 1 \qquad \phi_n^T \mathbf{B} \phi_n = \varpi_n^2 \qquad \phi_n^T \mathbf{D} \phi_n = 2\xi_n \varpi_n$$

Hence, the equation of motion corresponding to the *n*th mode of vibration can be written as follows:

$$\ddot{y}_n + 2\xi_n \varpi_n \dot{y}_n + \varpi_n^2 y_n = 0 \quad \text{n = i, p, o} \qquad (12)$$

The solution requires initial and boundary conditions associated with mandrel pop-out at the end of expansion process. Figure 1 shows the tube-fluid system where the tube is fixed at the bottom end and is free at the top end. Hence, the boundary conditions can be expressed as:

$$w_{n=i,\ o,\ p}(0,t) = 0, \qquad \text{at the } \textit{fixed end}$$

$$\left.\begin{array}{l} p_{n=i,\ o}(L,t) = 0 \\ \sigma_p(L,t) = 0 \end{array}\right\} \qquad \text{at the } \textit{free end} \qquad (13a)$$

During the expansion process, the tube is subjected to uniform axial stress, σ_p, inner pressure, q_i, and outer pressure, q_o, which is thereby independent of z. With the sudden release of the mandrel, the stress and pressure at the free end of the tube along with the inner and outer fluids drop to zero, leading to the following initial conditions:

$$\dot{w}_{n=i,\ o,\ p}(z,0) = 0$$

$$p_{n=i,\ o}(z \neq L,t) = q_n \qquad (13b)$$

$$\sigma_p(z \neq L,t) = \sigma_0$$

where $\dot{w}_n(z,0)$ represents the axial velocities of the three mediums. Using the initial and boundary conditions given in Eqn. 13, the solution for axial displacement, stress, and pressure within the three mediums can be expressed as follows:

$$w_n(z,t) = \sum_{k=1}^{\infty} \mathsf{A}_n^{(k)}(t)\sin\left(\frac{2k-1}{2L}\pi z\right)$$

$$p_n(z,t) = \sum_{k=1}^{\infty} \mathsf{B}_n^{(k)}(t)\cos\left(\frac{2k-1}{2L}\pi z\right) \qquad (14)$$

where n = i, p, o and k = 1, 2, 3, ..., oo,

$$\mathsf{A}_n^{(k)}(t) = \begin{cases} \dfrac{2(-1)^{k-1}q_n}{L\rho_n \varpi_n^{(k)2}}\left(\sqrt{\dfrac{\xi_n^{(k)2}}{1-\xi_n^{(k)2}}}\sin\omega_n^{(k)}t + \cos\omega_n^{(k)}t\right) \\ \qquad e^{-\xi_n^{(k)}\varpi_n^{(k)}t} \qquad \text{if } \xi_n^{(k)} < 1 \\ \dfrac{2(-1)^{k-1}q_n}{L\rho_n \varpi_n^{(k)2}}(1+\varpi_n t)e^{-\varpi_n^{(k)}t} \quad \text{if } \xi_n^{(k)} = 1 \\ \dfrac{2(-1)^{k-1}q_n}{L\rho_n \varpi_n^{(k)2}}\left(\dfrac{-\alpha_+}{\alpha_- - \alpha_+}e^{\alpha_- t} + \dfrac{\alpha_-}{\alpha_- - \alpha_+}e^{\alpha_+ t}\right) \text{if } \xi_n > 1 \end{cases}$$

and

$$\mathsf{B}_n^{(k)}(t) = \begin{cases} \dfrac{4q_n}{\pi}\dfrac{(-1)^{k-1}}{(2k-1)}\left(\cos\omega_n^{(k)}t - \sqrt{\dfrac{\xi_n^{(k)2}}{1-\xi_n^{(k)2}}}\sin\omega_n^{(k)}t\right) \\ \qquad e^{-\xi_n^{(k)}\varpi_n^{(k)}t} \qquad \text{if } \xi_n^{(k)} < 1 \\ \dfrac{4q_n}{\pi}\dfrac{(-1)^{k-1}}{(2k-1)}(1-\varpi_n t)e^{-\varpi_n^{(k)}t} \quad \text{if } \xi_n = 1 \\ \dfrac{4q_n}{\pi}\dfrac{(-1)^{k-1}}{(2k-1)}\left(\dfrac{-\alpha_+}{\alpha_- - \alpha_+}e^{\alpha_- t} + \dfrac{\alpha_-}{\alpha_- - \alpha_+}e^{\alpha_+ t}\right) \text{if } \xi_n > 1 \end{cases}$$

where $\alpha_\pm = \xi_n \varpi_n \pm \sqrt{\xi_n^2 - 1}$. Transforming the product functions in Eqn. 14 to summation functions using trigonometric and hyperbolic identities shows that each wave propagation equation consists of two terms. The first one represents a wave traveling in a forward $(z - c_n t)$ direction and the second in a backward $(z + c_n t)$ one. At any arbitrary location in the tube, the response will be determined by the superposition of forward and backward waves. These waves may overlap each other to reach an absolute maximum or attenuate to reach an absolute minimum, depending on the speed of the two waves. It is also important to note that each wave expression is an infinite sum of vibration modes. The contribution of each mode is inversely proportional to its wave number.

4. Results and Discussions

Once the mandrel pops out, the tube-fluid system is excited by the sudden release of energy stored in the

system. This initial excitation at the free end of the tube results in stress and pressure waves propagating in the three mediums. To investigate the dynamic effects of the pop-out phenomenon, a typical field case with an expansion ratio of 20% and a friction coefficient of 0.1 was considered. The geometrical and material parameters were the inner radius of the tube- $r_i = 0.0504$ m, outer radius of the tube- $r_o = 0.0635$ m, tube length- $L = 20$ m, wellbore radius- $r_w = 0.17$ m, Poisson's ratio- $v = 0.3$, Young modulus- $E = 206$ GPa, density of tube material- $\rho_p = 7800$ kg/m³, yield strength- $Y = 500$ MPa, bulk modulus of the inner and outer fluids- $B_i = B_o = 2.15$ GPa, densities of inner and outer fluids- $\rho_i = \rho_p = 1000$ kg/m³, and formation shear modulus- $G = 10.2$ GPa.

A conical shaped mandrel was used for expansion with an optimal cone angle of 20° (Pervez *et al.* 2005). In order to quantify the post-expansion system response, the drawing force required to expand the tube was determined using a finite element analysis (Pervez *et al.* 2005). At the end of the expansion process, the inner fluid pressure was 57 MPa and the axial stress in the tube was 149 MPa. These values then became the initial conditions for the tube-fluid system. The boundary conditions were governed by the fixed end condition at the bottom end of the tube.

4.1 Damping and Coupling Effects

The mathematical model developed in the previous section was used to determine the response of the damped system. An experiment conducted by Fossen and Johansen (2002) on an equivalent submerged structure measured the damping ratio as $\xi_p^{(1)} = 3\%$. Also for this particular case, it was found that the damping ratios for the first few modes were close to one another. Hence, using Eqn. 10, the constants $a_0 = 18.1$ and $a_1 = 3.37 \times 10^{-3}$ of the damping model were determined. The system response to the above-mentioned excitation can be written as a linear combination of the three vibration modes as given below:

$$\vec{R} = \left\{ 65.14\vec{V}_i + 149\vec{V}_p + 0.02\vec{V}_o \right\} MPa \qquad (15)$$

It is important to note that the superposition of the axial stress and displacement of the tube was allowed because the deformation in the z-direction was purely elastic [Appendix 6].

Figure 2 shows the waves propagating in the three mediums with respect to time and position along the z-axis of the tube. It can be seen that the tube experienced a high apparent frequency of 64 Hz as compared to the inner and outer fluid frequencies, which were

18.43 and 16.41 Hz, respectively. In terms of displacements, it can be seen in Figs. 2 (a), (c), and (e) that the inner and outer fluid tubes reached 0.6 m, 1.4 cm and 2.3 cm, respectively, when the mandrel popped out. In addition, Fig. 2 shows that the displacements satisfied the initial conditions defined by Eqn. 13. The displacements were maximized at the free end ($z = L$) and equal to zero at the fixed end ($z = 0$). It can also be noticed that the initial displacement of the inner fluid at the tube's free end was quite high as compared to the tube length (5%) but this result was expected with the high inner fluid pressure. Initially, the response corresponded to the excitation imparted to the system. Figures 2(b), (d), and (f) show that the inner and outer pressure and the axial stress were equal to 57 MPa, zero Pa and 149 MPa, respectively, when the pop-out took place. After pop-out, the displacements, stress, and pressures started decaying and interacting with each other as shown analytically by Eqn. 14. Also of note is that the amplitudes of the fluid pressures and tube axial stress were maximal at the fixed end ($z = 0$) of the system and equal to zero at the free end ($z = L$).

The developed mathematical model incorporates the coupling, which takes place only in the case of hydraulic expansion. It significantly affects the response of the tube-fluid system in terms of amplitudes, wave propagation speeds, and frequencies. The interactions between the wave-guide components largely depend on the geometry and material properties. The three eigenvalues are $\lambda_i = 12.07$, $\lambda_p = 1.001$ and $\lambda_o = 15.22$, and their corresponding wave propagation speeds are $s_i = 1.0055\sqrt{B_i/\rho_i}$, $s_p = 0.999\sqrt{E/\rho_p}$ and $s_o = 0.89\sqrt{B_o/\rho_o}$ for the inner fluid, tube, and outer fluid, respectively. The square root terms represent the sonic speed in each medium and their coefficients represent the coupling effect on the wave propagation speeds. In case of no coupling between three mediums, the coefficients will be unity.

Note that the inner fluid mode was slightly affected by the radial flexibility of the tube. The wave propagation speed increased by 0.5% relative to the sonic speed. The effect on the tube was almost negligible. However, the outer fluid mode was substantially affected and the wave propagation speed was lowered by 11% as compared to the corresponding uncoupled wave propagation speed. This was due to the low shear modulus of the formation and the radial flexibility of the tube. For each eigenvalue, λ, there was a corresponding eigenvector describing the contribution in terms of amplitude of each medium on the propagation modes. The three eigenvectors, as columns, are given in the following matrix:

Coupling and Damping Effects on the Dynamics of Submerged Expanded Tubes in Borehole Wells

(a) Axial displacement of the inner fluid

(b) Pressure of the inner fluid

(c) Axial displacement of the tube

(d) Axial stress of the tube

(e) Axial displacement of the outer fluid

(f) Pressure of the outer fluid
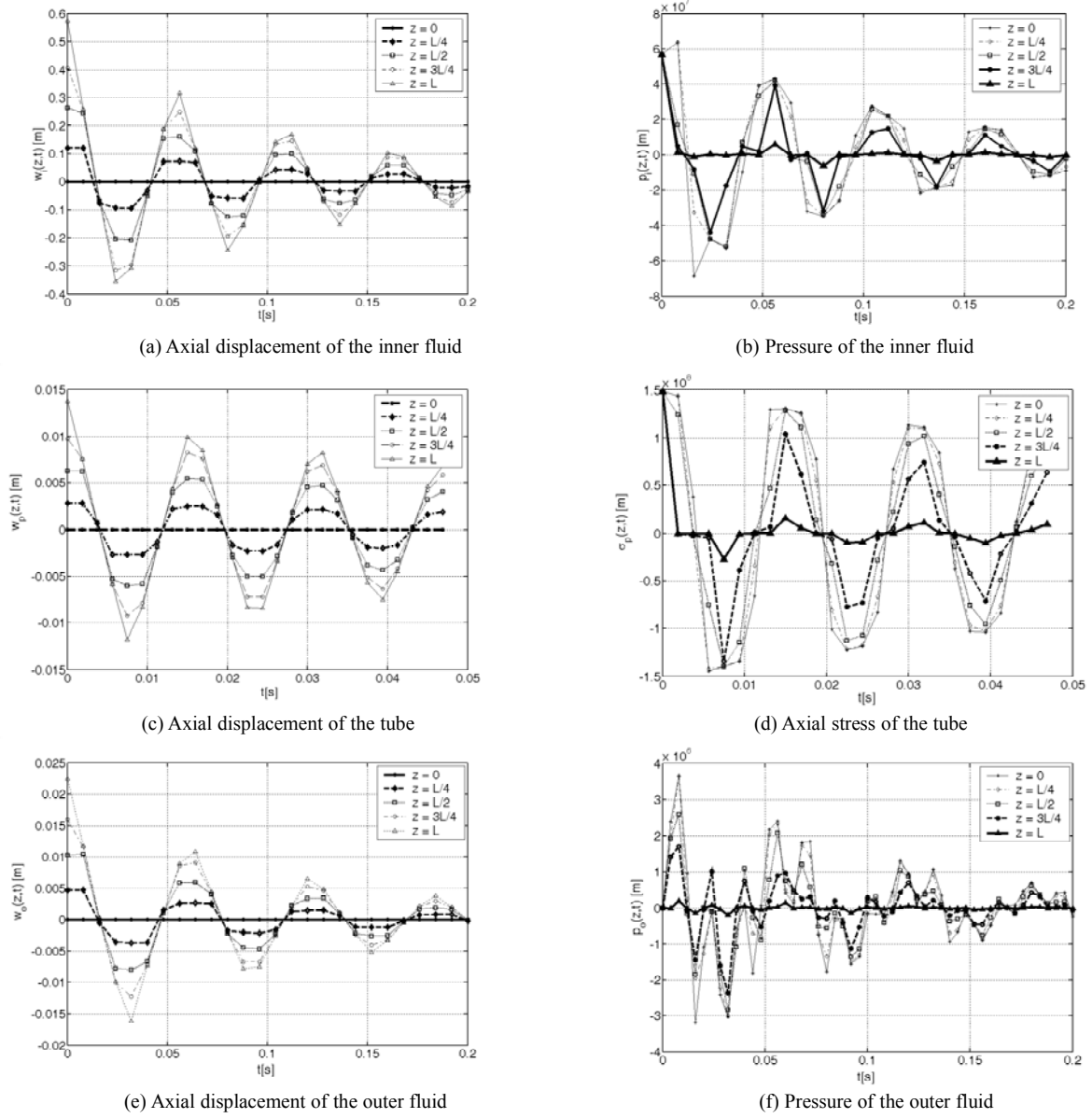
Figure 2. Response of tube-fluid system in terms of axial displacement, stress and pressures
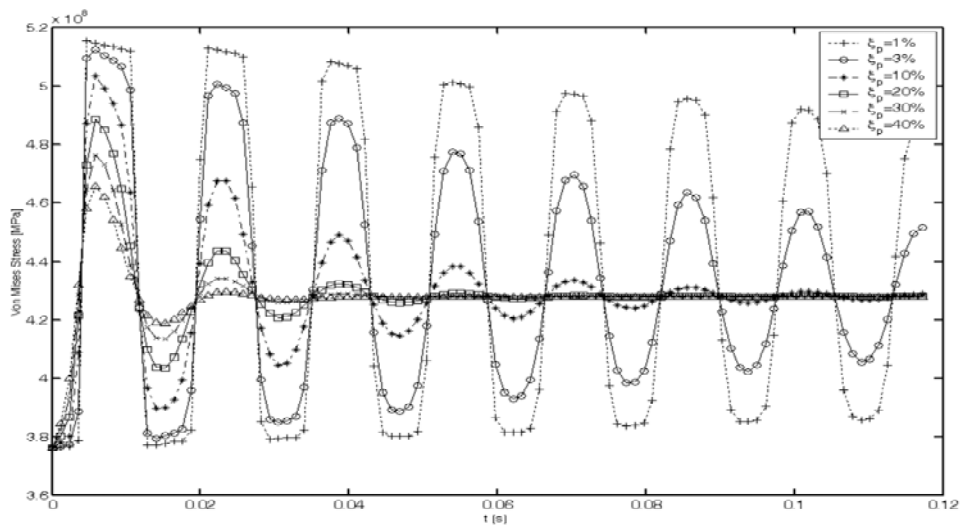
Figure 3. Von Mises stress variation versus time for different damping ratios (at the fixed end)

$$\mathbf{\Phi} = \begin{pmatrix} 1 & -0.0542 & -0.0156 \\ 0 & 1 & -0.0054 \\ 0 & -0.0137 & 1 \end{pmatrix} \qquad (16)$$

The eigenvectors were normalized in order to study the contribution of each medium to the others. It can be observed that the off-diagonal terms representing the coupling effect were, in general, small in magnitude. For example, in the second mode, a vibration amplitude of 1 mm in the tube induced a vibration amplitude of 0.0542 mm and 0.0137 mm in the inner and outer fluids, respectively. This means that each mode was strongly located within its own medium and the disturbances in other mediums were very small.

Interestingly, the inner fluid mode was contained within itself and did not produce any disturbances to the tube or outer fluid (two zeros in first column). This is due to the elastic perfectly plastic tube material. The inner fluid was in contact with the plastic region of the tube, while the outer fluid was in contact with the elastic region.

The effective stress at various locations along the tube length and at different times was calculated for different damping ratios. Figure 3 shows that at the fixed end of the fluid tube system, the maximum effective stress decreased with the increase in damping ratio. Figure 4 shows the distribution of the effective stress along the tube with respect to time, at different damping ratios. Therefore, it can be deduced that the most critical region is in the neighborhood of the tube-fluid system fixed end. For instance, the system under consideration was characterized by a damping ratio of $\xi_p^{(1)} = 3\%$. The effective stress of this particular case increased from an initial value of 375 MPa and reached yield strength between t = 0.005s and t = 0.01s after mandrel pop-out. It means that the tube experienced local yielding near the fixed end. The same behavior was observed when $\xi_p^{(1)} = 20\%$ and $\xi_p^{(1)} = 30\%$ but with different absolute maximums of 490 MPa and 470 MPa, respectively. For relatively high damping ($\xi_p^{(1)} > 10\%$,) the effective stress reaches a maximal stress value and starts vibrating, but does not reach the yield strength of the tube. Therefore, it can be concluded that the structural failure due to pop-out occurs in the neighborhood of the tube fixed end at low damping ratios. This results in a more than required expansion of the tube in the vicinity of the fixed end, leading to a larger localized deformation known as ballooning. The ballooning of the tube near the fixed end is not desirable for two reasons. First, it will result in varying tube diameters near

each fixed end, which is not acceptable to operators. Second, it will create a converging-diverging nozzle in between the tube and formation, when a series of expanded tubes are joined together to construct a mono-diameter well. Consequently, the nozzle effect will create excessive vibration of the tube during operation. Since the stress wave propagates back and forth, and the damping is relatively low, the effective stress will again exceed material yield strength. Hence the pop-out will weaken the structural integrity of the tube unless inherent system damping damps out the excessive energy or external damping measures are incorporated based on operating procedure. A corrective addition of damping would be needed in order to preserve the structural integrity.

The changes in the fluid properties of the outer fluid due to the presence of mud will enhance the inherent system damping.

4.2 Effects of Geometrical and Material Properties

The response of the formation-fluids-tube system is highly influenced by the material properties and geometry. The objective of this section is to study the effects of the formation shear modulus and tube stiffness on the response of the structure in terms of natural frequency and coupling between the propagating waves.

Figures 5 (a) and (b) show that the natural frequencies and wave propagation speeds increase with tube stiffness. It is important to note that according to Eqns. 15 and 16, the predominant mode of system vibration corresponds to the tube. Therefore, the components of this mode are reported in Fig. 6, which shows that the coupling effects vanish with an increase in tube rigidity. This result was expected as the coupling effects are mainly related to the stiffness of the tube and formation as can be seen through Eqns. 9 through 11. When the stiffness of the tube increases, the cross-sectional change of the inner and outer fluid medium reduces. This results in less interaction between the three mediums.

On the other hand, it can be seen in Figs. 7 (a) and 8 (a) that the frequency of the tube and the interaction between the tube and inner fluid do not change significantly with the formation shear modulus. However, the frequency of the outer fluid and the amplitude of the coupling term between the outer fluid and tube increase with the formation shear modulus, as shown in Figs. 7 (b) and 8 (b). This means that in the predominant mode of vibration, the component associated with the annulus is much more affected by the formation shear modulus variation than the others. This phenomenon is equivalent to the garden hose effect where larger hoses yield lower fluid speeds. Moreover, when the stiffness of the formation increases, the amount of

Coupling and Damping Effects on the Dynamics of Submerged Expanded Tubes in Borehole Wells
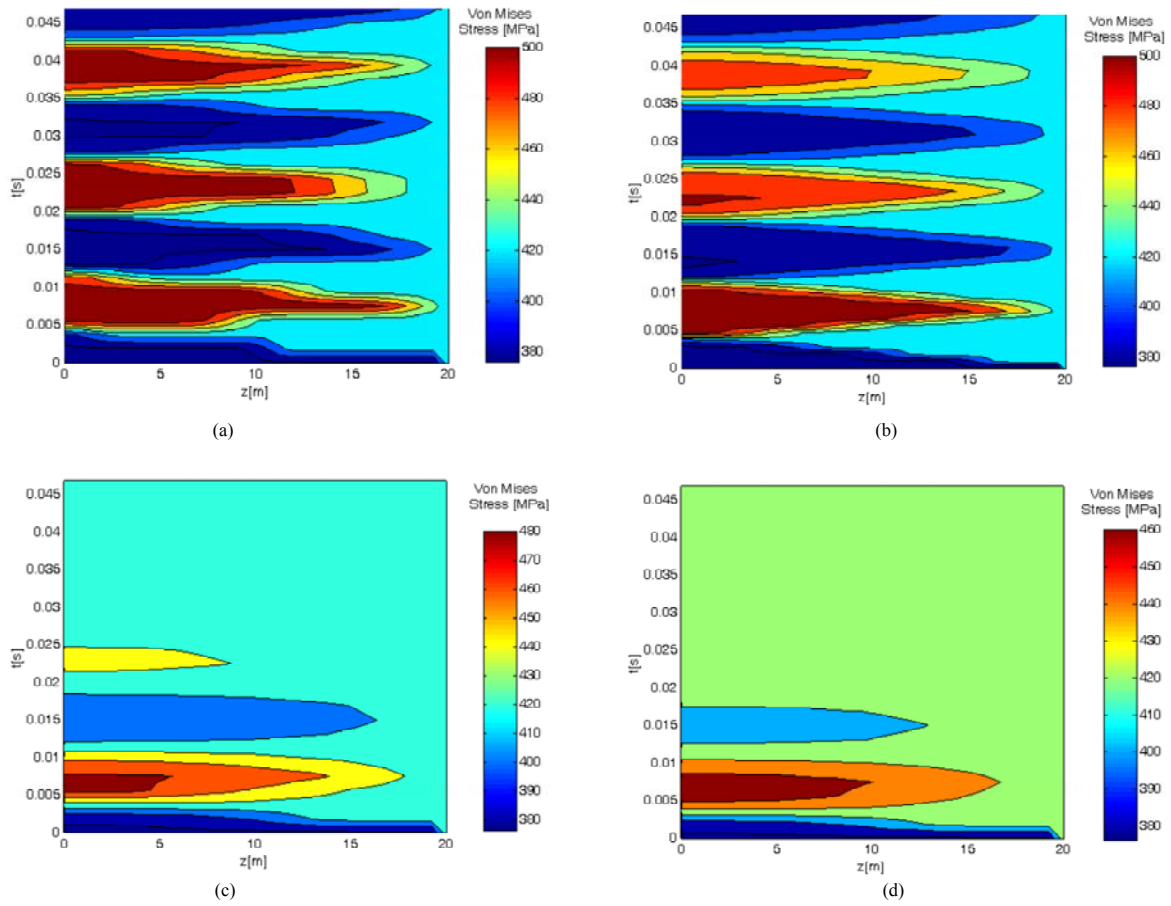
Figure 4. von Mises stress variation versus time, at the fixed end for different damping ratios
(a) $\xi^{(1)}_p = 1\%$; (b) $\xi^{(1)}_p = 3\%$; (c) $\xi^{(1)}_p = 20\%$ and (d) $\xi^{(1)}_p = 30\%$
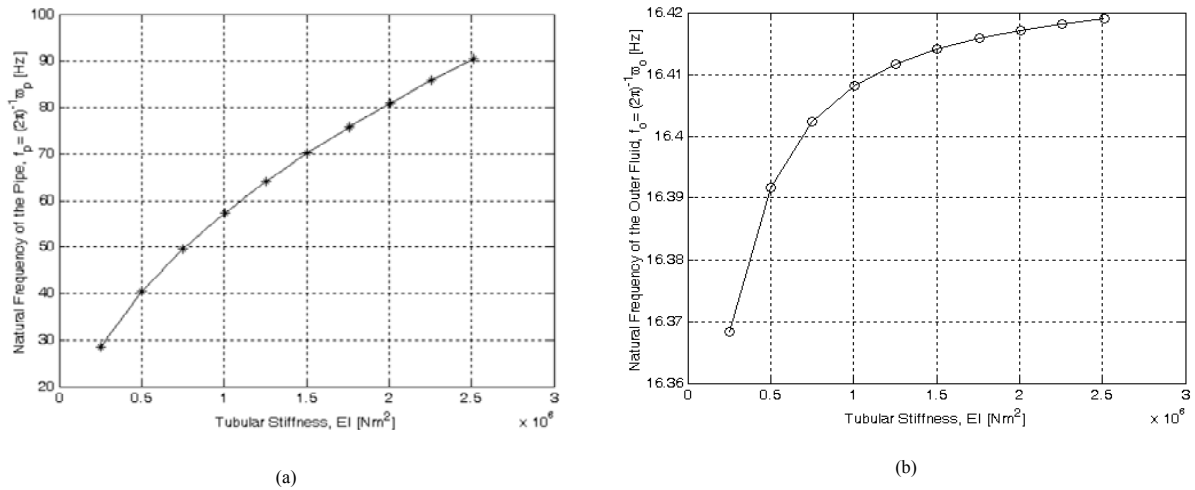
Figure 5. Variation of the tube (a) and outer fluid (b) frequencies with respect to the tube stiffness

20

A Karrech and AC Seibi
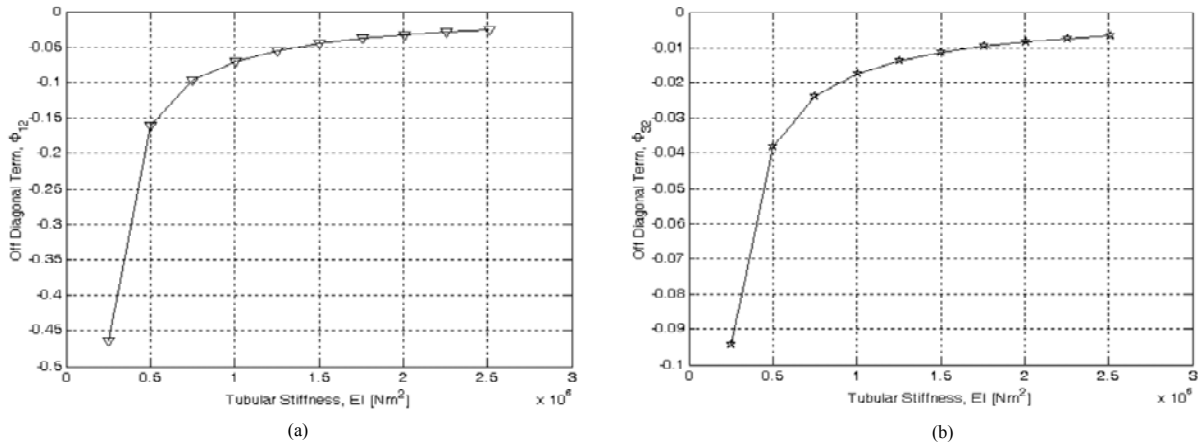
Figure 6. Variation of the first (a) and third (b) components of the predominant mode of vibration with respect to the tube stiffness
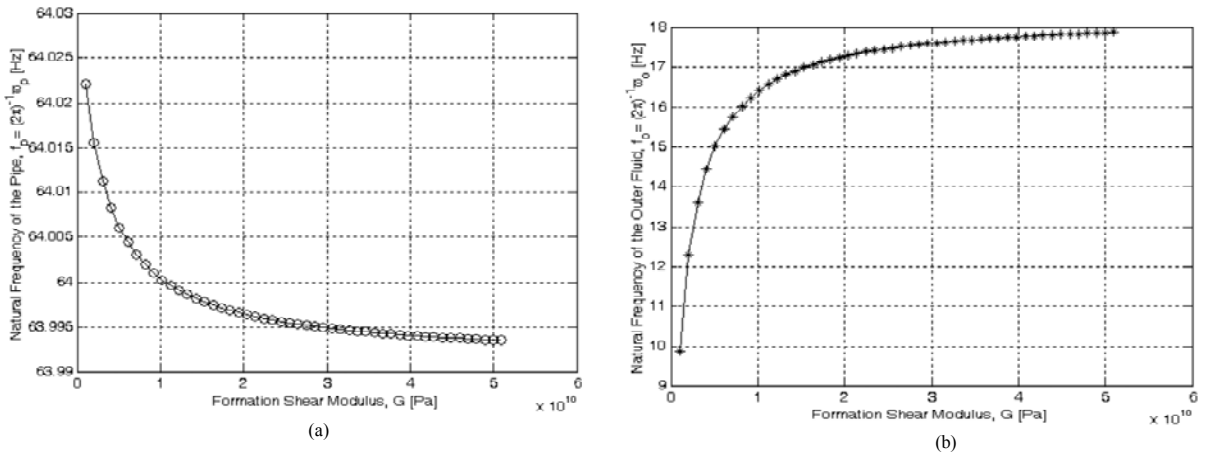
Figure 7. Variation of the tube (a) and outer fluid (b) frequencies with respect to the formation shear modulus
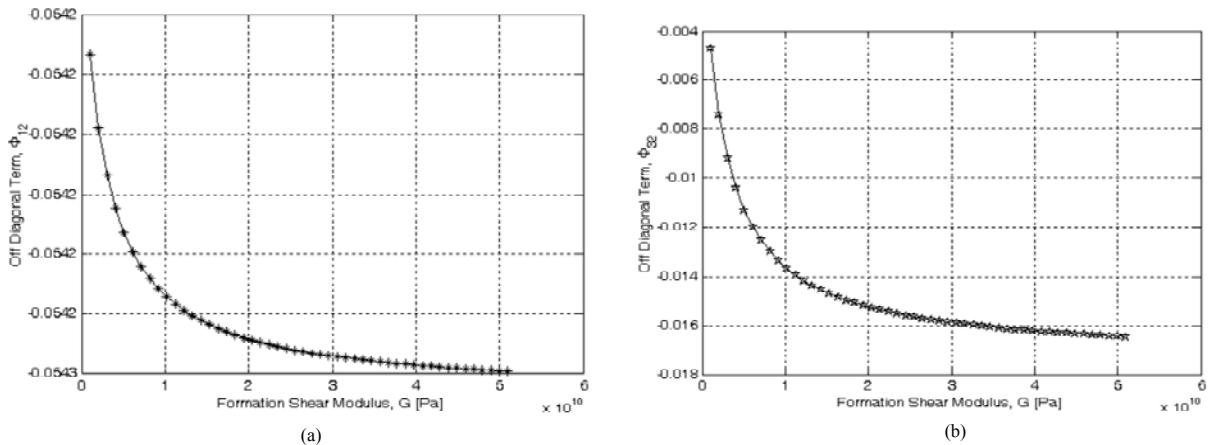
Figure 8. Variation of the first (a) and third (b) components of the predominant mode of vibration, with respect to the formation shear modulus

energy imparted to three mediums does not perform work on the formation. This increases the amplitudes of the waves in the outer-fluid-tube region.

5. Conclusions

A mathematical model for tubes submerged in inner and outer fluids inside boreholes was developed

to investigate the dynamics of fluids and expanded tubes due to the input energy imparted to the system at the end of the expansion process. This model took into consideration the damping as well as the coupling effects. An analytical solution was obtained for the displacement, and for the stress and pressure wave propagation. It was found that the expanded tube has a localized critical region in the vicinity of the fixed end of the tube, which, under the right conditions, may fail. The inherent system damping helps to reduce the failure, but it is not enough to completely avoid it. An alternative solution is to provide external corrective damping in the system, which would be costly and difficult to implement in field conditions. Furthermore, a sensitivity analysis was conducted in order to study the effects of the geometry and the formation material properties on the response of the system in terms of frequency, wave propagation speeds. and coupling effects. The sensitivity analysis showed that the fundamental frequency of the outer fluid varied significantly with the formation shear modulus. But the tube fundamental frequency was insensitive to variation in the formation shear modulus. The reverse was true when tube stiffness varied. More studies would be required to study the use of solid expandable tube technology in drilling mono-diameter wells efficiently with less cost and time. Future work may also include other aspects such as the formation porosity or the non-conservativity of the fluid mediums at the end of the expansion process.

References

Aarrestad TV, Tonnesen HA, Kyllingstad A (1986), Drill string vibrations: Comparison between theory and experiment on a full-scale research drill rig. SPE Paper # 14760, 9-12 February 1986, IADC/SPE Drilling Conference, USA.

Apostal MC, Haduch GA, Williams JB (1990), A study to determine the effect of damping on finite-element-based, forced-frequency-response models for bottom-hole assembly vibration analysis. SPE Paper # 20458, 23-26 September 1990, Annual Technical Conference and Exhibition of SPE.

Daigle CL, Campo DB, Naquin CJ, Cardenas R, Ring LM, York PL (2000), Expandable tubulars: Field examples of application in well construction and remediation. SPE Paper # 62958, 1-4 October 2000, SPE Annual Technical Conference and Exhibition, Dallas, Texas, USA.

Filippov A, Mack R, Cook L, York P, Ring L, McCoy T (1999), Expandable tubular solutions. SPE Paper # 56500, 3-6 October, 1999, SPE Annual Technical Conference and Exhibition, Houston, Texas, USA.

Fossen TI, Johansen TA (2002), Hydro launch free decay tests. NTNU Rapport 2001-18-T.

Mark R, Filippov A, Kendziora L, Ring L (2000), In-situ expansion of casing and tubing - Effect on mechanical properties and resistance to sulfide stress cracking. NACE International. NACE 00164, March 26-31 2000, Orlando, Florida, USA.

Karrech A, Seibi AC, Pervez T, Al-Hiddabi S (2004), Stress/Fluid pressure waves in radially expanded solid tubular. 12th Annual PVPD Student Paper Competition, 25-29 July 2004, ASME Pressure Vessels and Piping Division Conference 473:101-111.

Lea SH (1996), Propagation of coupled pressure waves in borehole with drill string. SPE Paper # 37156, 18-20 November 1996, International Conference on Horizontal Well Technology.

Owoeye O, Leste O, Aihevba RA, Hartmann VC (2000), Optimization of well economics by application of expandable tubular technology. IADC/SPE Paper # 59142, 23-25 February 2000, IADC/SPE Drilling Conference, New Orleans, Louisiana. USA.

Pervez T, Seibi AC, Karrech A (2005), Simulation of solid tubular expansion in well drilling using finite element method. Journal of Petroleum Science and Technology 23:775-794.

Prevez T, Seibi AC, Karreach A (2006), Analytical solution for wave propagation due to pop-out phenomenon in solid expandable tubular system. Journal of Petroleum Science and Technology 24:923-942.

Ruggier M, Scott B, Urselmann R, Mossor H, Van NR (2001), Advances in expandable tubing - A case history. SPE/IADC Paper # 67768, 27/2/ 1001 to 1 March 2001, SPE/IADC Drilling Technology Conference, Amerterdam, Netherlands.

Seibi A, Karrech A, Pervez T, Al-Hiddabi S (2004), Finite element modeling of solid tubular expansion in well engineering. TSS International Conference on Advances in Mechanical Engineering (ICAME 2004), March 2004, Sousse, Tunisia.

Seibi A, Al-Hiddabi S, Pervez T, Karrech, Al-Yahmadi A, Al-Shabibi A (2003), Simulation of pop-out phenomena in wellbore expandable tubular. Petroleum Development Oman. Project No CR/ENG/MIED/01/23, September 2004, Phase III.

Stewart RB, Marketz F, Lohbeck WM (1999), Wellbore expandable tubulars. SPE Paper # 60799, SPE Technical Symposium, 16 October 1999, Dhahran, Saudi Arabia.

Wang X, Bloom F (1999), Dynamics of a submerged and inclined concentric pipe system with internal and external flows. Journal of Fluids and Structures 13:443-460.

Appendix

Wave propagation in fluids both inside and outside the tube

The conservation of mass and momentum of a fluid element, inside and outside the tube, leads to the following equations of motion:

$$\frac{\partial}{\partial t}(\rho A) = -\frac{\partial}{\partial z}(\rho A v) \tag{A-1}$$

$$\frac{\partial}{\partial t}(\rho A v) = -\frac{\partial}{\partial z}\left(\rho A v^2\right) - A\frac{\partial p}{\partial z} \tag{A-2}$$

By neglecting the convective terms and using simple algebraic transformations, (A-1) and (A-2) can be reduced to the following form:

$$\frac{\rho}{B}\frac{\partial^2 w}{\partial t^2} - \frac{\partial^2 w}{\partial z^2} = \frac{1}{A_0}\frac{\partial A}{\partial z} \tag{A-3}$$

$$\rho\frac{\partial^2 w}{\partial t^2} = -\frac{\partial p}{\partial z} \tag{A-4}$$

where B is the bulk modulus defined by $B = \rho(dp/d\rho)$, ρ is the fluid density, p is the fluid pressure, A_0 is the initial section, and w is the axial fluid displacement. A-3 shows that for very stiff tubes and/or formations, the wave equation reduces to an uncoupled problem since the cross-sectional change, $\frac{\partial A}{\partial z}$, is negligible. This means that the coupling effect is largely related to the radial displacement of the solid layers (*ie.* the tube and the formation).

Governing equation for wave propagation in the tube

The effects of fluid viscosity are negligible. This means that there are no shear stresses either at the inner or outer surface of the tube. Therefore, using an infinitesimal tube element, the equations of motion for the tube in the cylindrical coordinate system (r, θ, z) can be expressed as

$$\frac{\partial \sigma_r}{\partial t} + \frac{\sigma_r - \sigma_\theta}{r} = \rho_p \frac{\partial^2 u}{\partial t^2} \tag{A-5}$$

$$\frac{\partial \sigma_z}{\partial z} = \rho_p \frac{\partial^2 w}{\partial t^2} \tag{A-6}$$

where u and w denote the radial and axial displacements. Since the internal fluid pressure developed during the post-expansion process is uniform along the tube, the plastic zone is delimited by a cylindrical surface of radius c, which is independent of z. Considering Tresca's yield criterion and a harmonic solution for the radial displacement, it can be shown that the radial and hoop stresses in the elastic region $c \leq r \leq r_o$ are governed by the following equations:

$$\frac{\sigma_r}{Y} = \frac{c^2}{2} \left\{ \frac{1}{r_o^2} - \frac{1}{r^2} \right\} - \frac{p_0}{Y}$$

$$\frac{\sigma_\theta}{Y} = \frac{c^2}{2} \left\{ \frac{1}{r_o^2} + \frac{1}{r^2} \right\} - \frac{p_0}{Y}$$

(A-7)

where Y is the yield strength. In the plastic region ($r_i \le r \le c$), the stresses satisfying the tube equation of motion and Tresca's yield criterion can be written as

$$\frac{\sigma_r}{Y} = -\frac{1}{2} - Ln\frac{c}{r} + \frac{c^2}{2 r_o^2} - \frac{p_o}{Y}$$

$$\frac{\sigma_\theta}{Y} = \frac{1}{2} - Ln\frac{c}{r} + \frac{c^2}{2 r_o^2} - \frac{p_o}{Y}$$

(A-8)

According to Tresca's yield criterion, the onset of yielding is given by the yield function $f(s) = \sigma_\theta = \sigma_r = Y$. The plastic strain increment can be expressed as follows, using Levy's flow rule:

$$d\varepsilon_p = d\zeta \frac{df}{d\sigma}$$

(A-9)

where $d\varepsilon_p$ is the plastic strain increment and $d\zeta$ is a scalar factor of proportionality which varies with the deformation. The equation in Appendix 9 gives $d\varepsilon_\theta^p = -d\varepsilon_r^p$ and $d\varepsilon_z^p = 0$, which indicates that the axial strain is purely elastic. The constitutive relationships between the stresses and the strains can be written as

$$E\varepsilon_z = \sigma_z - \nu(\sigma_r + \sigma_\theta)$$

(A-10)

$$E(\varepsilon_r + \varepsilon_\theta) = (1-\nu)(\sigma_r + \sigma_\theta) - 2\nu\sigma_z$$

(A-11)

By integrating the previous equation and using the continuity of the displacement between the plastic and the elastic zone, it can be deduced that

$$\frac{u}{r} = -\nu\varepsilon_z + \frac{(1-2\nu)(1+\nu)}{E} s_r + Y\frac{(1-\nu^2)}{E}\frac{c^2}{r^2}$$

(A-12)

Using the constitutive relationship (A-10) and the equation of motion of a cylindrical element in the axial direction of equation (A-6), the axial displacement can be expressed as

$$\frac{E}{\rho_p}\frac{\partial^2 w_p}{\partial z^2} = \frac{\partial^2 w_p}{\partial t^t} - \frac{2\nu}{\rho_p}\frac{\partial p_o}{\partial z}$$

(A-13)

Substitution of the relation between fluid and pressure (A-4) into the equation in A-13 results in a final equation of motion for the wave propagation in the tube as in Eqn 2:

$$\frac{E}{\rho_p}\frac{\partial^2 w_p}{\partial z^2} = \frac{\partial^2 w_p}{\partial t^t} - \frac{2\nu\rho_o}{\rho_p}\frac{\partial^2 w_o}{\partial t^2}$$

(A-14)

The second term of the right hand side of A-14 represents the coupling effect between the outer fluid and tube displacements. In the absence of outer fluids, it is obvious that A-14 reduces to the classical wave equation in solids. Using the expression in A-12, the derivative of the radial displacement with respect to z for the inner and the outer surface of the tube can be expressed as

$$\frac{1}{r}\frac{\partial u}{\partial z} = -\nu\rho_p \frac{\partial^2 w_p}{\partial t^2} + \frac{1-2\nu}{2G}\frac{\partial s_r}{\partial z} \tag{A-15}$$

In the fluid layers, the axial motion is governed by A-3; the right hand term of that equation represents the dynamic change of the cross-sectional area either for the inner or outer fluids. Inside the tube, this dynamic change is due to the radial displacement of the inner surface and is approximated by $\frac{1}{A_0}\frac{\partial A}{\partial z} \approx \frac{\partial u_i}{\partial z}$. Using the constitutive equation relating the hoop strain, the stresses, and the boundary condition $\sigma_{r|r=r_i} = -p_i$, the axial motion of the fluid inside the tube can be written as follows (Eqn. 1):

$$\frac{B_i}{\rho_i}\frac{\partial^2 w_i}{\partial z^2} = \left(1 + \frac{(4\nu^2 + 2\nu - 1)B_i}{E}\right)\frac{\partial^2 w_i}{\partial t^2} + 2\nu\frac{\rho_p}{\rho_i}\frac{B_i}{E}\frac{\partial^2 w_p}{\partial t^2} - 4\nu^2\frac{B_i}{E}\frac{\rho_o}{\rho_i}\frac{\partial^2 w_o}{\partial t^2} \tag{A-16}$$

By neglecting the second order term of the tube axial displacement at the outer radius and expressing the radial displacement of the borehole wall $u_b \approx \frac{r_b p_o}{2G}$, the equation of motion of the outer fluid can be written as follows (Eqn. 3):

$$\frac{E}{\rho_p}\frac{\partial^2 w_o}{\partial z^2} = \frac{2\nu r_o^2}{r_o^2 - r_b^2}\frac{\partial^2 w_p}{\partial t^2} + \left(\frac{E}{B_o} + \frac{r_b^2 E G^{-1} + 2(1-\nu)r_o^2}{r_b^2 - r_o^2}\right)\frac{\rho_o}{\rho_p}\frac{\partial^2 w_o}{\partial t^2} \tag{A-17}$$

where G is the shear modulus of the formation.